AMS Bologna
Internal Note
2005–03–01

Single light guide efficiencies of the AMS-02 TOF counters. Comparison between simulation and measurement.

Diego Casadei[1]
INFN, Sezione di Bologna, Via Irnerio 46, 40126 Bologna, Italy

Gianluca Massaccesi
Via Banchieri 27, 40133 Bologna, Italy

March 8, 2005

ABSTRACT

In order to find the best distribution of the AMS-02 TOF photomultiplier tubes, it is necessary to know the effective light guide efficiency for all scintillator counters. A ray-tracing simulation has been carried on with 12 different counters, in order to better understand the experimental results obtained in the INFN Bologna laboratories using cosmic rays. The simulated and the measured light guide efficiencies are discussed.

Subject headings: light guide, ray-tracing, efficiency.

1. Introduction

The superconducting magnet of the AMS-02 detector [1] produces a strong fringing field where the photomultiplier tubes (PMTs) of the TOF system are installed (figure 1). In order to reduce the effect of the magnetic field on PMTs (figure 2), a special kind of tube has been chosen (Hamamatsu R4956 "fine mesh" PMT) and special effort was devoted to design the light guides (LGs) of the TOF scintillation counters in order to minimize the relative angle between the **B** vector and the PMT axis (figure 3).

The LGs consist of:

1. a small piece of plexyglass with a circular face (coupled to the PMT window through a soft transparent silicon pad) opposed to a rectangular face (figure 4). The latter is glued to
2. an optional piece of plexyglass with rectangular ends and a curved geometry (figure 5). If present, this piece is glued to
3. the scintillator or the scintillator "extender" (a plexyglass extension to the scintillator paddle). A counter with all LGs is shown in figure 6.

The first short piece of the LG can be directly glued to the scintillator or to its extender, constituting the whole LG. The second piece of plexyglass has different shapes for different counters, for a total of six different geometries. These pieces are obtained by bending and possibly twist-

[1]Diego.Casadei@bo.infn.it

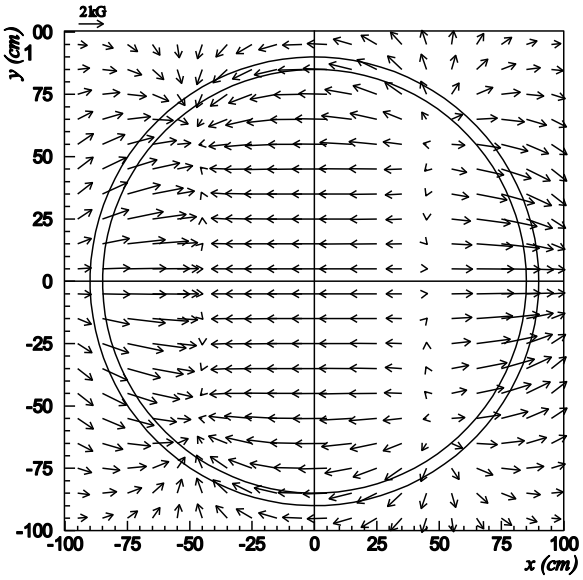

Figure 1. Magnetic field on TOF PMTs.

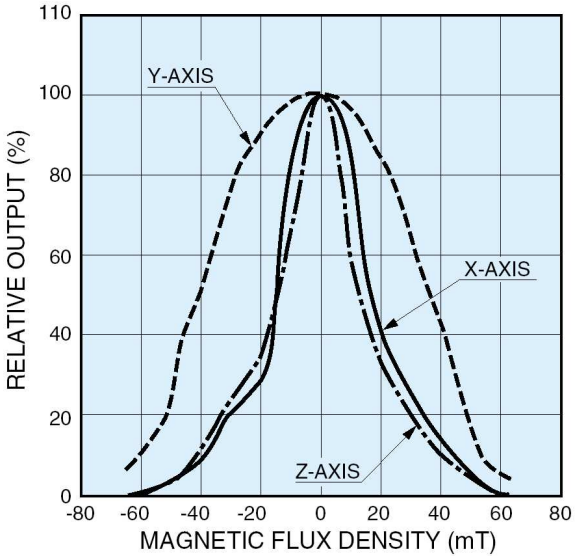

Figure 2. The effect of magnetic field on common PMTs.

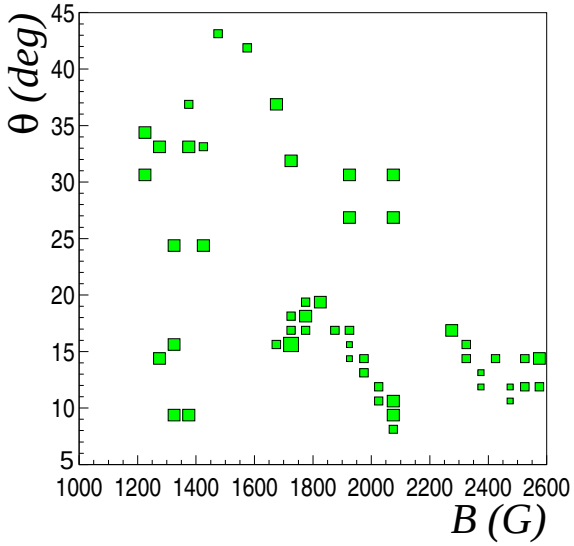

Figure 3. The TOF field-PMT angle distribution as function of the magnetic field intensity.

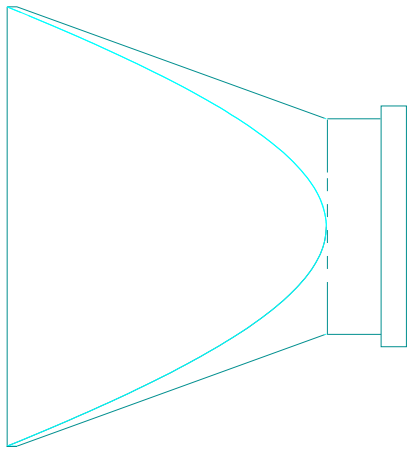

Figure 4. The first short LG piece connects the circular PMT window (to be placed on the right) to the glued rectangular surface (left face).

ing a straight piece of plexyglass, as schematically shown in figure 5.

Compared to the shortest LGs (consisting only of the first piece), the transmission efficiency of the other LGs is lower: the LG geometry effectively reduces the phase space of the photons. The reduction of the light intensity due to the longer path (hence larger absorption) can be neglected in comparison with the geometrical effect: the bulk attenuation length in plexyglass is of the order of 3 m, whereas the linear dimensions of each LG complex are lower than 0.2 m.

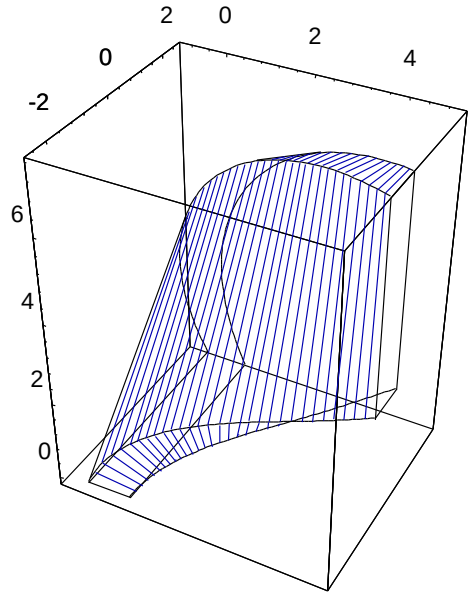

Figure 5. Example of curved and bended geometry (not a real shape for final TOF LGs) [2].

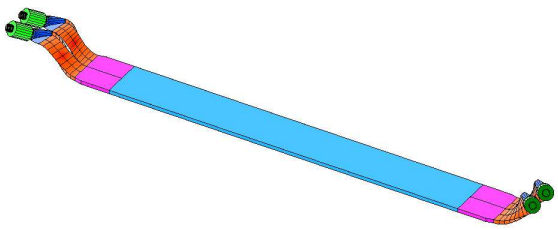

Figure 6. Final configuration of a TOF counter with curved LGs.

2. Ray-tracing simulation

In order to compute the response of the different LG types, a ray-tracing simulation has been carried on with several configurations, using the CAD project of the TOF counters of planes 3 and 4 (figure 7). The ray-tracing technique is an application of the geometrical optics: given a point source and its light intensity in the 3D space, where geometrical objects with given optical properties (refractive indices) are placed, single light rays are generated uniformly over a sphere centered on the source, and they are traced

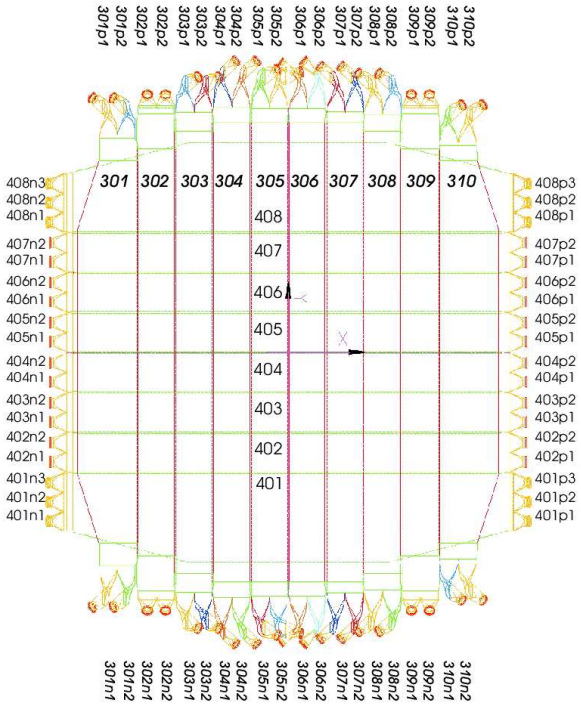

Figure 7. Naming conventions for PMTs in lower TOF planes.

until they stop or reach the target surface.

The first task was to adequately simulate the input light source for the LGs. From measurements carried on with AMS-01 TOF counters [3], it is known that particles crossing the scintillator at least 15 cm far from the LG glueing generate light that is equally collected by the LGs installed at the same counter side. Hence, in order to get a realistic illumination of the scintillator exit surface, a linear uniform light source[2] was put in the center of the scintillator, 50 cm away from the exit surface. Being this distance the same for all simulated LG configurations, the results are independent from the attenuation length of the scintillator and LGs.

The simulation was carried on in steps. First, the linear uniform source was used to get the light

[2] In practice, 101000 point sources of unit intensity were uniformly distributed along a vertical 1 cm long track crossing the scintillator paddle.

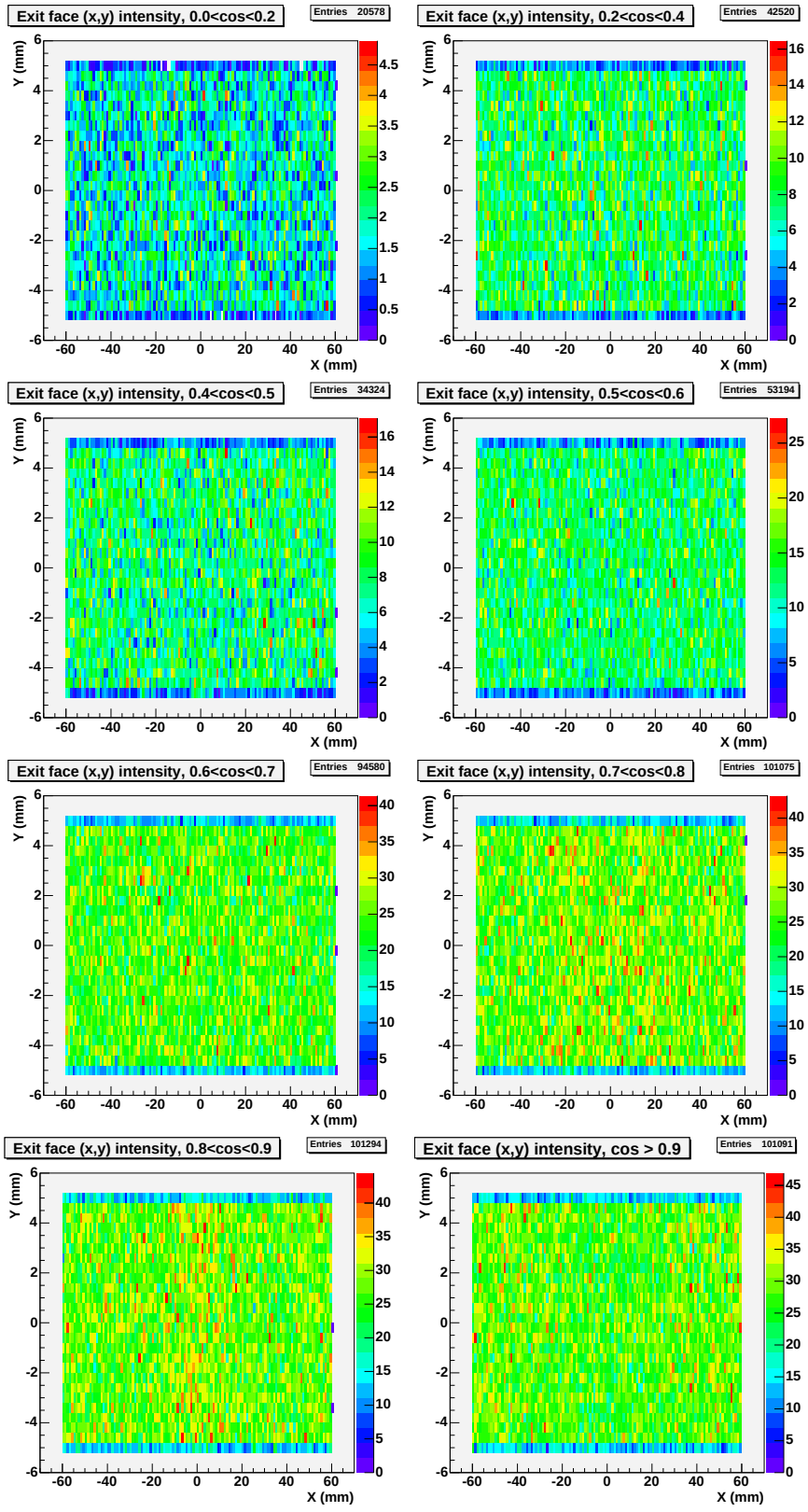

Figure 8. Intensity maps at the scintilator output, for different exit angles.

distribution on the exit surface of the scintillator (figure 8). For each light ray reaching this surface, the crossing position, its intensity and incoming direction were saved in a text file (7 floating point numbers per ray). This file was used as the source for the simulation of all LG configurations but the trapezoidal scintillators (counters 401 and 301), for which a uniform linear source in the mid of the scintillator, 50 cm away from its exit surface, was used[3]. In this way, one can easily compare the results of all configurations.

The light distribution on the scintillator exit surface was then used as the input for the simulation of the LGs of counter 402, that are short and straight (2 cm long extender[4] glued to two short pieces). This counter was taken as reference: the light intensity at the exit from its LGs was defined as "100% intensity". Its systematic uncertainty, defined as the difference between the results obtained for the two identical 402 LGs, was approximated (by excess) to 1%.

For all other configurations, the LGs consist of both the first short piece and of the intermediate curved piece. The simulation was carried on step by step, saving on separate files the light distribution corresponding to all interfaces. In this way it was possible to get information about the effects of each intermediate piece. During analysis, data on each file were displayed as intensity maps over the corresponding exit surface, using the same $\cos\theta$ binning as figure 8 (0–0.2, 0.2–0.4, 0.4–0.5, 0.5–0.6, 0.6–0.7, 0.7–0.8, 0.8–0.9, 0.9–1, plus $\cos\theta < 0$ to find reflected light).

As an example, figure 9 shows the histograms of the unit vector components relative to the extender of counter 302, figure 10 shows the intensity maps of the light exiting from the interface between the first and the curved pieces of a LG of counter 302, and figure 11 shows the intensity maps of the light exiting from the first piece of the corresponding PMT.

3. Analysis of the simulation results

Let us defines the *absolute efficiency* as the ratio between the exit intensity and the input intensity of the linear source. Though the overall normalization is uncertain because of the attenuation effects[5], it makes sense to compare the absolute efficiencies of all configurations (the trapezoidal counters included).

On the other hand, the *relative efficiency* is defined as the ratio between the exit intensity of each configuration and the average output intensity of the two LGs of counter 402, taken as reference. The relative efficiencies are more meaningful for all configurations (with a possible exception for counters 301 and 401), because they do not depend on the bulk light attenuation.

In particular, for counters 301 and 401 the assumption that the computed efficiency is the same for all particles crossing the counter farther than 15 cm from the glueing of the LGs may not be valid. Their shape is not symmetrical with respect to a 180° rotation about the longitudinal axis, hence in general the fraction of collected light by each LG can depend on the flash position. As table 1 shows, the effect is a $\sim$ 10% reduction of the light seen by the outermost PMT (401n1, see figure 7), compared to the other two PMTs, which receive the same intensity within few percent. The systematic uncertainties associated to all curved LGs were computed as the absolute difference between the output intensities of the two (max – min for counter 401) LGs installed on the same counter side.

The results for all configurations are also shown in figure 12, where the absolute (left panel) and relative (right panel) efficiencies are plotted.

[3] The shape of such scintillators is not symmetrical under a 180° rotation around the longitudinal axis, hence the linear source was not seen centrally by the LGs.

[4] Actually, the real 402 counter has no extender. Instead, the scintillator section is reduced in the last 2 cm to match the area of the two small LGs. Because the refractive index is the same, this makes no difference.

[5] For all materials in the simulation the bulk attenuation length was set to 3 m.

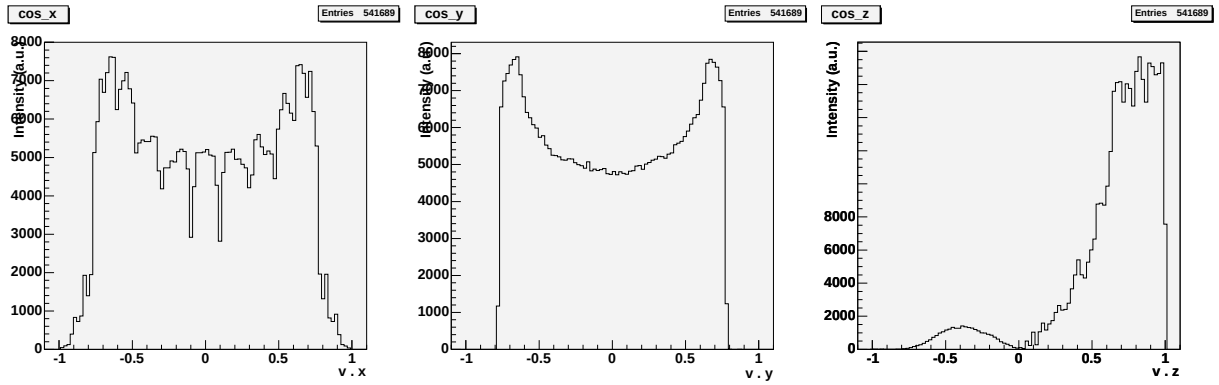

Figure 9. Distribution of the exit light ray unit vector components, for the extender of the counter 302.

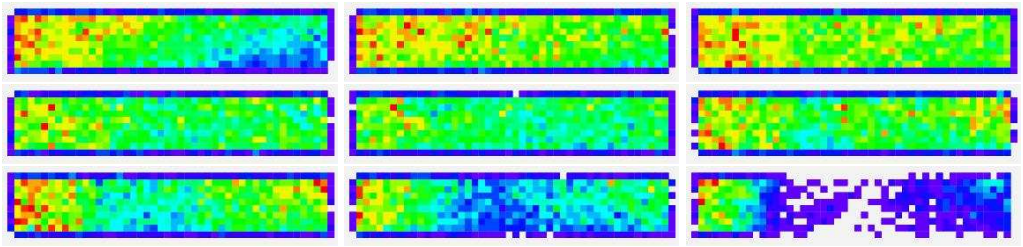

Figure 10. Intensity maps of the curved LG piece of PMT 302n2. The first map (top left panel) refers to reflected light ($\cos\theta < 0$), and the following ones, left to right, refer to $\cos\theta$ binning: 0–0.2, 0.2–0.4, 0.4–0.5, 0.5–0.6, 0.6–0.7, 0.7–0.8, 0.8–0.9, 0.9–1 (lowest right panel).

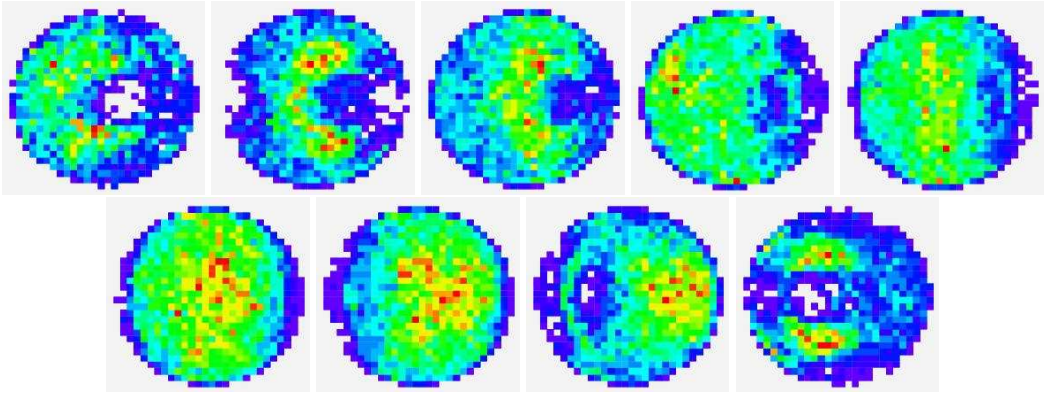

Figure 11. Intensity maps of the first piece of PMT 302n2. The first map (top left panel) refers to reflected light ($\cos\theta < 0$), and the following ones, left to right, refer to $\cos\theta$ binning: 0–0.2, 0.2–0.4, 0.4–0.5, 0.5–0.6, 0.6–0.7, 0.7–0.8, 0.8–0.9, 0.9–1 (lower right panel).

In addition to the total exit intensity, the intensity of the light rays forming smaller angles than 60° with the normal to the PMT window is also shown. Because for larger angles the photoelectric conversion efficiency of the PMT photocathode can be neglected, the latter is more meaningful when compared to measured data.

	Absolute efficiency (%)				**Eff. (%) rel. to scint./ext.**				**Eff. (%) relative to ⟨402⟩**			
	Total		**(< 60°)**		**Total**		**(< 60°)**		**Total**		**(< 60°)**	
PMT	value	err.	value	err.	value	err.	value	err.	value	err.	value	err.
301n1	4.40	0.28	3.83	0.24	10.7	0.7	9.3	0.6	77.1	4.8	78.4	5.0
301n2	4.13		3.59		10.1		8.7		72.3		73.4	
302n1	4.99	0.05	4.25	0.04	12.2	0.1	10.4	0.1	87.4	0.9	86.9	0.8
302n2	5.04		4.29		12.3		10.5		88.3		87.7	
303n1	4.05	0.17	3.50	0.14	9.9	0.4	8.5	0.3	71.0	3.0	71.6	2.9
303n2	4.23		3.64		10.3		8.9		74.0		74.5	
304n1	4.47	0.57	3.87	0.48	10.9	1.4	9.4	1.2	78.3	9.9	79.1	9.7
304n2	3.90		3.39		9.5		8.3		68.4		69.4	
305n1	4.44	0.28	3.84	0.26	10.8	0.7	9.4	0.6	77.7	4.9	78.5	5.3
305n2	4.16		3.58		10.1		8.7		72.8		73.2	
306n1	4.03	0.07	3.51	0.11	9.8	0.2	8.6	0.3	70.5	1.2	71.8	2.2
306n2	4.09		3.62		10.0		8.8		71.7		74.0	
307n1	4.39	0.08	3.81	0.06	10.7	0.2	9.3	0.2	77.0	1.3	77.9	1.3
307n2	4.32		3.74		10.5		9.1		75.7		76.6	
308n1	4.35	0.32	3.82	0.30	10.6	0.8	9.3	0.7	76.1	5.6	78.1	6.2
308n2	4.03		3.52		9.8		8.6		70.5		72.0	
309n1	5.01	0.11	4.26	0.08	12.2	0.3	10.4	0.2	87.8	1.9	87.2	1.7
309n2	5.12		4.34		12.5		10.6		89.7		88.8	
401n1	1.23	0.20	1.09	0.17	4.7	0.8	4.2	0.7	21.6	3.5	22.3	3.5
401n2	1.41		1.21		5.4		4.6		24.6		24.8	
401n3	1.43		1.26		5.5		4.8		25.1		25.8	
402n1	5.70	0.01	4.88	0.03	13.89	0.03	11.88	0.07	99.88	0.24	99.70	0.60
402n2	5.72		4.90		13.93		11.95		100.12		100.30	
⟨402⟩	*5.71*	*0.01*	*4.89*	*0.03*	*13.91*	*0.03*	*11.91*	*0.07*	*100.0*	*0.24*	*100.0*	*0.6*

Table 1. Simulated efficiencies. Errors were computed as the difference between maximum and minimum values obtained at the same side, hence are the same for all PMTs in this side. The last row shows the reference values, i.e. the average of the two PMTs of counter 402.

The LGs of counter 310 are not covered by the analysis, because of corrupted data. However, their configuration is very similar to that of counter 301, hence their efficiency should be almost the same as for counter 301.

4. Measurements

A characterization of all AMS-02 flight TOF counters was carried on in the INFN Bologna laboratories, using the same four PMTs [4].

A short initial run was done using a fixed set of voltages for these PMTs, before equalizing their response for minimum ionizing particles (MIPs) vertically crossing the scintillators at their center.

Whereas the anode signals of the PMTs placed on the same counter side are passively summed before reaching the charge integrator, dynode signals are read independently for each PMT. Counters with curved LGs were operated with nominal PMT gains larger by a factor of 3 than those used for the counters of planes 1 and 4, which all have straight and short LGs.

The initial runs (with fixed HV settings) can

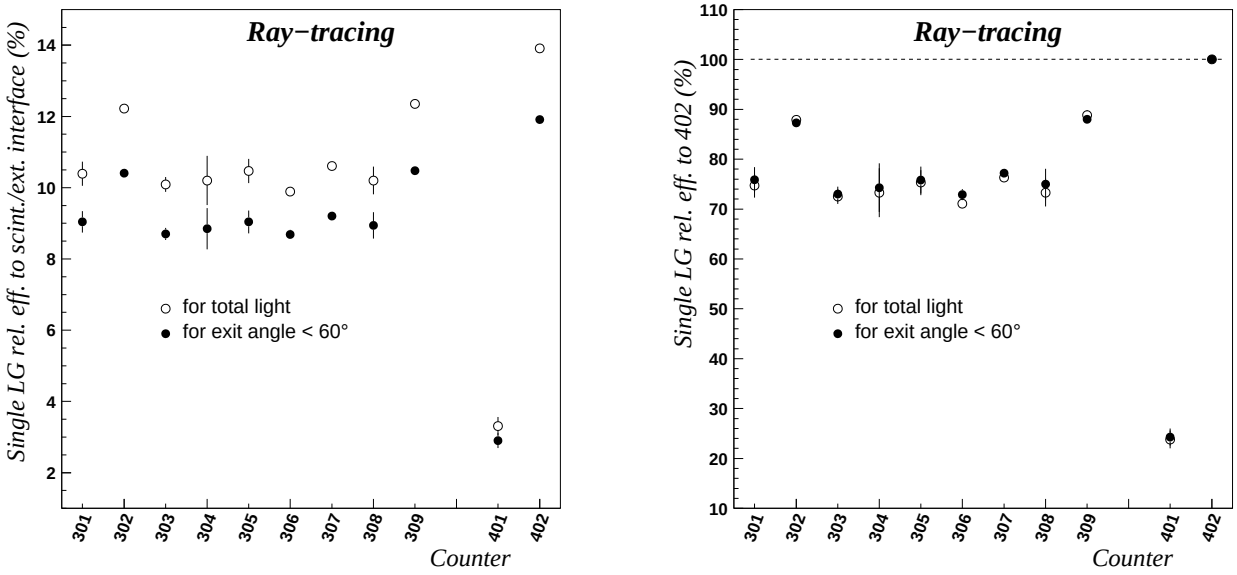

Figure 12. Simulated single light guide efficiency (open circles), computed as the ratio between the average intensity of the light exiting from the two (three for counter 401) LGs and the intensity of the light exiting from the rectangular section of the scintillator (*left plot*) and normalized to the average efficiency of counter 402 (*right plot*). The same quantities are also shown when exiting rays form a smaller angle than 60 degrees with the surface unit vector (full circles).

be used to compute the relative efficiency of each LG, considering only dynode signals. This was done for all counters with 4 LGs and for the corresponding channels of the counters with 6 LGs (101, 108, 401, 408). Experimental data are available on the AMS Bologna Group web site[6]; data taken until October 7, 2004 were considered in this work.

Measured data refer to peak positions corresponding to MIPs crossing the central slice of all counters. Hence the difference in the counter length (13 cm between the shortest and longest counters) will in principle systematically decrease the efficiency of longer counters. The maximum effect can be easily estimated to be roughly equal to 4%, of the same order of magnitude of the standard deviation of repeated measurements with the same counter (see below) and of the measurements carried on with equal counters (102–107 and 402–407). Hence we don't expect to be able to see this effect in experimental data.

First, let us look at the repeated measurements carried on with the same counter (406), installed 6 times in the experimental setup to test the repeatability of the results. The RMS fluctuation of the four channels are:

Channel	**Peak** (pC)	**RMS** (pC)	**RMS** (%)
d1n	3.69	0.10	3
d2n	3.97	0.59	15
d1p	2.28	0.18	8
d2p	2.02	0.21	10

where "d1n" is the first dynode of the negative counter side, et cetera.

The big spread is mostly due to the last measurement (measurement "406*" in the following table), taken after the characterization of all counters, which can be omitted to get:

[6] `http://ams.bo.infn.it`

Ch.	**Peak** (pC)	**RMS** (pC)	**RMS** (%)	**406* – Peak** (pC)
d1n	3.66	0.08	2	0.18
d2n	4.20	0.12	3	−1.42
d1p	2.27	0.19	8	0.11
d2p	1.96	0.14	7	0.40

(apart from channel d1p, the differences between 406* and the mean of the previous five measurements of counter 406 are sensibly larger than the fluctuations).

Neglecting measurement 406*, the effective gain[7] stability ranged from 2% to 8%.

Because the analog signals produced by counters with curved light guides is quite small, all such counters were characterized using PMT gains that were nominally three times higher than for counters with short and straight light guides. The actual values for the gain ratios were determined making use of the double measurement carried on with the counter 404 and the two sets of HV settings:

	Ratio G3/G1	
Ch.	**Value**	**Error**
d1n	2.70	0.11
d1p	3.38	0.37
d2n	2.59	0.79
d2p	2.70	0.26

(these values will be used to scale the response of all counters to the same gain).

Then, the problem is to correlate the results obtained with different channels, i.e. to find the relative normalization between different PMTs (for all measurements, the PMT-channel pairs were ZH7119-d1n, ZH7610-d1p, ZH7651-d2n, ZH5789-d2p). This could be done by looking at the repeated measurements of counter 404, which was positioned in all possible combinations PMT-LG. Taking (arbitrarily) channel d1p as reference, the following ratios can be found:

[7]The effective gain, in addition to the PMT gain, takes also into account the effect of the optical coupling between PMT and LG, through a transparent and soft silicon pad.

	2p/1p	**1n/1p**	**2n/1p**
Average	1.27	1.44	0.87
Std.dev.	0.04	0.11	0.08
Std.dev. (%)	2.9	7.5	9.3

where “d1p” has been set to 1.00 and its spread has been found to be 4%. However, it comes out that the efficiencies obtained this way look very low and have a big spread.

Thus a different technique has been used in this paper to equalize the measurements done with different PMTs. For each channel (i.e. PMT), the measured peak position was rescaled to the gain used for counters of planes 1 and 4, then its maximum amplitude was taken as the reference peak. Finally, all peak positions were divided by the corresponding reference value, obtaining the relative efficiencies for each channel. The assumption here is that the highest value of each channel should be equal to the 100% efficiency within the measurement uncertainty.

The result is shown in table 2, where two PMTs per side are not included for counters 101, 108, 401 and 408. It comes out that the highest amplitudes were measured for the counters 402 (d2p, ±7.1%), 404 (d1p, ±8.4%), 406 (d1n, ±2.2%), and 407 (d2n, ±2.7%). No single counter was seen to have more than one reference signal.

Counters might be affected by problems related to the LG glueing. In addition, the counter preparation procedure might occasionally fail in obtaining a good optical contact between the PMT, the soft silicon pad and the LG. In these (hopefully rare) cases, one should get efficiencies very low with respect to the averaged value. Hence, in order to find potential problems, the best way is to look for counters with anomalous efficiency on a single channel (assuming that the probability to have two bad LGs is low). In order to make this task easier, the last four columns of table 2 show the averaged efficiency ϵ over the four measurement channels, the ratio between their standard deviation σ_ϵ and their average ϵ, the difference Δ between maximum and mini-

mum values, and its relative importance Δ/ϵ, respectively. Good counters should have a small dispersion σ_ϵ/ϵ of measured efficiencies and a relatively small difference Δ between the maximum and minimum values.

Before looking the details of table 2, let us make a consistency check. Comparing counters 102–107 (identical) and 402-207 (with the same geometry, but 3.5 cm = 2% longer than 102–107), one would expect to measure the same efficiencies within their uncertainties (peak positions are known with roughly 5% uncertainty). Actually, the averaged efficiencies over the plane 4 counters are consistent with this hypothesis. Quoting [average; standard deviation] pairs: $\langle$d1n$\rangle_4$ = [90; 7]%, $\langle$d2n$\rangle_4$ = [90; 9]%, $\langle$d1p$\rangle_4$ = [94; 6]%, $\langle$d2p$\rangle_4$ = [88; 9]%. However, the same averages for the plane 1 show larger fluctuations (though they have smaller errors) and a systematic decrease for the p-side: $\langle$d1n$\rangle_1$ = [89; 4]%, $\langle$d2n$\rangle_1$ = [93; 3]%, $\langle$d1p$\rangle_1$ = [84; 7]%, $\langle$d2p$\rangle_1$ = [75; 7]%. This means that the computed errors are probably underestimated in many cases.

Table 2 shows that side p is systematically lower than side n for counters 102, 104, 202, 203, 204, 205, 206, 207 and 307, whereas the contrary happens for counters 310 and 402 only. Counters with an anomalous high single channel efficiency are 101 (d2p), 108 (d2p), 404 (d1p, used as reference), 407 (d2n, used as reference), and 408 (d2p). It is possible that these measurements are affected by some systematic effect.

Too low efficiencies, that would be expected to correspond to optical problems, are found for counters 103 (d2p!), 105 (d2p), 205 (d1p!), 206 (d1p! and d2p!), 309 (d1p!), 401 (d2n!), 402 (d2n), 407 (d2p), 408 (d1n!). In addition, channel d1p is a bit low for counters 208, 303, 304 and 305.

REFERENCES

[1]The AMS Collaboration (J. Alcaraz et al.), "The Alpha Magnetic Spectrometer (AMS)", NIM A 478 (2002) 119-122.

[2]D. Casadei, "Light Propagation in Curved Light Guides", AMS Bologna Int. Note 2000-01-01, Jan 17, 2000.

[3]D. Casadei, "Esperimento AMS: problemi teorici e sperimentali nella ricerca di antimateria in raggi cosmici", tesi di laurea, Università di Bologna, 1998.

[4]F. Giovacchini, L. Quadrani, C. Sbarra, "TOF light guides efficiency", AMS Bologna Int. Note 2005-01-25, Jan 25, 2005.

	d1n		**d1p**		**d2n**		**d2p**					
Counter	**eff.**	**err.**	**eff.**	**err.**	**eff.**	**err.**	**eff.**	**err.**	ϵ	σ_ϵ/ϵ	$\Delta\epsilon$	Δ/ϵ
	(%)	(%)	(%)	(%)	(%)	(%)	(%)	(%)	(%)		(%)	
101	20.9	0.8	23.6	3.4	22.8	1.5	36.0	3.5	25.8	0.27	15.1	0.59
102	88.3	2.0	76.6	6.4	91.2	2.5	80.1	5.7	84.1	0.08	14.6	0.17
103	94.4	2.1	91.0	7.7	96.2	2.6	64.2	4.5	86.5	0.17	32.0	0.37
104	91.7	2.0	73.9	6.2	94.2	2.6	71.8	5.1	82.9	0.14	22.4	0.27
105	87.4	2.0	91.0	7.7	94.9	2.6	73.6	5.2	86.7	0.11	21.3	0.25
106	86.6	1.9	84.2	7.1	88.2	2.4	79.2	5.6	84.6	0.05	9.0	0.11
107	84.1	1.9	85.7	7.2	95.8	2.6	82.4	5.8	87.0	0.07	13.4	0.15
108	14.3	0.6	18.2	2.6	17.7	1.2	32.6	3.1	20.7	0.39	18.3	0.88
201	31.4	1.2	27.7	4.0	31.7	2.1	31.4	3.0	30.6	0.06	4.0	0.13
202	33.3	1.3	18.3	2.6	33.3	2.2	22.7	2.2	26.9	0.28	15.0	0.56
203	32.2	1.3	24.8	3.6	32.1	2.1	29.0	2.8	29.5	0.12	7.4	0.25
204	32.5	1.3	21.1	3.0	33.4	2.2	24.4	2.4	27.9	0.22	12.3	0.44
205	82.1	1.8	57.8	4.9	88.3	2.4	70.7	5.0	74.7	0.18	30.5	0.41
206	86.8	1.9	59.5	5.0	80.5	2.2	66.7	4.7	73.4	0.17	27.3	0.37
207	77.6	1.7	65.6	5.5	86.2	2.4	68.4	4.8	74.5	0.13	20.6	0.28
208	31.8	1.3	26.9	3.9	31.2	2.0	33.8	3.3	30.9	0.09	6.9	0.22
301	34.7	1.4	30.9	4.5	31.7	2.1	33.7	3.3	32.8	0.05	3.8	0.12
302	35.7	1.4	28.7	4.1	29.3	1.9	32.3	3.1	31.5	0.10	7.0	0.22
303	30.2	1.2	25.5	3.7	32.3	2.1	32.9	3.2	30.2	0.11	7.4	0.25
304	31.7	1.3	24.4	3.5	31.2	2.0	32.2	3.1	29.9	0.12	7.8	0.26
305	32.0	1.3	25.3	3.7	32.7	2.1	33.5	3.2	30.9	0.12	8.2	0.27
306	28.9	1.1	28.1	4.1	31.1	2.0	32.9	3.2	30.3	0.07	4.8	0.16
307	28.7	1.1	24.5	3.5	30.5	2.0	25.5	2.5	27.3	0.10	6.0	0.22
308	33.5	1.3	31.2	4.5	29.3	1.9	37.2	3.6	32.8	0.10	7.9	0.24
309	24.6	1.0	18.2	2.6	30.9	2.0	34.8	3.4	27.1	0.27	16.6	0.61
310	28.3	1.1	34.6	5.0	28.0	1.8	35.7	3.4	31.7	0.13	7.7	0.24
401	15.3	0.6	16.0	2.3	6.7	0.4	32.4	3.1	17.6	0.61	25.7	1.46
402	89.4	2.0	99.6	8.4	78.0	2.1	100.0	7.1	91.8	0.11	22.0	0.24
403	80.8	1.8	93.4	7.9	87.2	2.4	84.6	6.0	86.5	0.06	12.6	0.15
404	82.2	1.8	100.0	8.4	82.9	2.3	84.9	6.0	87.5	0.10	17.8	0.20
405	93.4	2.1	93.8	7.9	96.9	2.7	92.4	6.5	94.1	0.02	4.5	0.05
406	100.0	2.2	91.8	7.7	96.5	2.6	93.0	6.6	95.3	0.04	8.2	0.09
407	89.9	2.0	84.8	7.1	100.0	2.7	73.7	5.2	87.1	0.13	26.3	0.30
408	11.1	0.4	17.9	2.6	14.2	0.9	27.2	2.6	17.6	0.40	16.1	0.91

Table 2. Measured efficiencies. Last four columns show the averaged efficiency ϵ over the four measurement channels (two PMTs per side are not included for counters 101, 108, 401 and 408), the ratio between their standard deviation σ_ϵ and their average ϵ, the difference Δ between maximum and minimum values, and its relative importance Δ/ϵ, respectively.